

Removal of lead (II) and nickel (II) ions from aqueous solution using activated carbon prepared from rapeseed oil cake by Na_2CO_3 activation

Suat Uçar · Murat Erdem · Turgay Tay · Selhan Karagöz

Received: 17 March 2014 / Accepted: 3 August 2014 / Published online: 15 August 2014
© Springer-Verlag Berlin Heidelberg 2014

Abstract In this study, rapeseed oil cake as a precursor was used to prepare activated carbons by chemical activation with sodium carbonate (Na_2CO_3) at 600 and 800 °C. The activated carbon with the highest surface area of $850 \text{ m}^2 \text{ g}^{-1}$ was produced at 800 °C. The prepared activated carbons were mainly microporous. The activated carbon having the highest surface area was used as an adsorbent for the removal of lead (II) and nickel (II) ions from aqueous solutions. The effects of pH, contact time, and initial ion concentration on the adsorption capacity of the activated carbon were investigated. The kinetic data of adsorption process were studied using pseudo-first-order, pseudo-second-order kinetic models and intraparticle diffusion model. The experimental data were well adapted to the pseudo-second-order model for both tested ions. The adsorption data for both ions were well correlated with Langmuir isotherm. The maximum monolayer adsorption capacities of the activated carbon for the removal of lead (II) and nickel (II) ions were determined as 129.87 and 133.33 mg g^{-1} , respectively.

Keywords Activated carbon · Rapeseed oil cake · Adsorption · Chemical activation

Introduction

Heavy metal pollution is one of the world's most important environmental issues since heavy metals show high toxicity due to their solubility in water and easily accumulation in living organisms. Heavy metal contamination in wastewater is generated from various industrial processes such as mining, iron and steel, painting, and battery manufacturing (Giraldo-Gutierrez and Moreno-Pirajan 2008; El-Ash-toukhya et al. 2008). In contrast to the organic pollutants, heavy metals are not degradable, and they must be removed from wastewater. Accumulation of toxic heavy metals in human body can give serious damages to brain, kidney, liver, nervous system, red blood cells, lungs, nose, and bone. Thus, the concentration of toxic heavy metals in the industrial effluents and drinking water must be brought down to acceptable levels.

There are many conventional methods used for the removal of heavy metals from wastewater. These methods include chemical precipitation, electrochemical reduction, ion-exchange, evaporation, membrane filtration, reverse osmosis, ultra filtration, and adsorption (Patterson 1985; Singh et al. 2008; Amin et al. 2012). Among them, adsorption process has widely been used since it is not only effective but also economic process. There are various adsorbents such as synthetic polymers (Haroun et al. 2013; Haroun and El-Halawany 2011) and natural polymers (Kardam et al. 2014), zeolites (Merrikhpour and Jalali 2013), fly ash (Visa et al. 2011), various biomasses (Hebeish et al. 2011; Chouchene et al. 2014), and activated carbon (Nethaji and Sivasamy 2014) which have been used for the removal of heavy metals and dyes from wastewater. Among them, activated carbon is one of the best adsorbents in wastewater treatment as it is highly porous and low-cost material. There are two activation processes (physical and

S. Uçar (✉)
Chemistry Technology Program, Izmir Vocational School,
Dokuz Eylül University, 35160 Izmir, Turkey
e-mail: suat.ucar@deu.edu.tr

M. Erdem · T. Tay
Department of Chemistry, Faculty of Science, Anadolu
University, 26470 Eskişehir, Turkey

S. Karagöz
Department of Polymer Engineering, Faculty of Technology,
Karabük University, 78050 Karabük, Turkey

chemical) available to produce activated carbon. The physical activation is carried out into two steps. In the first step, called carbonization step, the precursor is carbonized. In the second step, called activation step, the carbonized materials are exposed to the activation with an oxidizing gaseous agent such as carbon dioxide, water vapor, or their mixture. In contrast to physical activation, chemical activation is performed at one step. In this process, activation and carbonization are united. The precursor is impregnated with a chemical reagent, and then the impregnated material is carbonized at desired temperature. Various chemicals (i.e., sodium hydroxide, sodium carbonate, potassium hydroxide, potassium carbonate, zinc chloride, phosphoric acid, and sulfuric acid) are used as chemical agents for the activation. Activated carbon can generally be prepared from both non-renewable sources such as coal (Zhang et al. 2012), and renewable sources like biomass (Ioannidou and Zabaniotou 2007). Agricultural by-products have widely been used as raw materials to prepare activated carbon since they are not only low-cost but also renewable materials. Some of agricultural by-products, which have been used as precursors for the preparation of activated carbon, are sugar cane husk (Giraldo-Gutierrez and Moreno-Pirajan 2008), sawdust (Ismadji et al. 2005), hazelnut husk (Imamoglu and Tekir 2008), almond husk (Hasar 2003), rice husk (Yalçın and Sevinç 2000), apricot stone (Sentorun-Shalaby et al. 2006), cassava peel (Sudaryanto et al. 2006), walnut shell (Nethaji and Sivasamy 2014), pomegranate peel (El-Ashtoukhya et al. 2008), and oil cakes (Bacaoui et al. 2001; Cimino et al. 2005; Karagoz et al. 2008).

In the present study, we report the preparation and characterization of activated carbons from rapeseed oil cake using sodium carbonate (Na_2CO_3) activation. The activated carbon with the highest surface area was used for the removal of lead (II) and nickel (II) ions from aqueous solutions. The effects of various parameters (i.e., pH, contact time, and initial ion concentration) on the adsorption capacities for lead (II) and nickel (II) ions were investigated. The kinetic data of the adsorption process for both ions were studied using different kinetic models. Langmuir and Freundlich isotherm models for adsorption of both ions onto activated carbon were also tested.

Experimental section

Materials

Rapeseed oil cake was used as a precursor without any treatment to prepare activated carbons in the study. It was supplied from Altınyaz vegetable oil company in Izmir. The elemental composition of the raw material was as follows; 45.92 wt % C, 6.21 wt % H, 6.90 wt % N, 0.88

wt % S, and 40.09 wt % O (by difference). The volatile matter, fixed carbon, and ash contents of the raw material were 77.90, 15.80, and 6.30 wt %, respectively. The component analysis of the raw material was also carried out according to a previous method (Li et al. 2004). The rapeseed oil cake on a dry basis contained 19.40 wt % extractives, 41.40 wt % hemicellulose, 4.99 wt % lignin, and 28.58 wt % cellulose. All chemicals and solvents used in the present study were purchased from Sigma Aldrich and used without any further purification.

Preparation of the activated carbons

Rapeseed oil cake as a precursor was used to produce activated carbon in the present study. First, rapeseed oil cake was impregnated with different Na_2CO_3 solutions for 24 h under continuous agitation (1,000 rpm). The impregnation ratio was fixed to 1.0 which refers to 100 wt % reagent concentration. The mixture was dried at 110 °C for 24 h. After that, the obtained samples were exposed to the carbonization process at 600 and 800 °C for 1 h under an inert atmosphere. The inert atmosphere was provided using nitrogen gas. The details about carbonization reactor and experimental set-up can be found in a previous report (Karagoz et al. 2008). After carbonization process, the samples were boiled with a hydrochloric acid solution (12 wt %) under reflux for 4 h in order to remove impurities and reduce ash contents of the activated carbons. Then, the products were washed several times with hot distilled water and then with cold distilled water until chloride ions were not detected. The obtained activated carbons were dried at 110 °C for 24 h.

In this study, the bio-chars were produced with carbonization of the rapeseed oil cake without any chemical activation at 600 °C (RAC1) and 800 °C (RAC2). The activated carbons produced from rapeseed oil cake with Na_2CO_3 activation at 600 and 800 °C were denoted as RAC3 and RAC4, respectively. Calculation for the chemical recovery of Na_2CO_3 activation process was carried out according to a previous report (Karagoz et al. 2008).

The following equation was used to calculate the yields of activated carbons and bio-chars based on the weight of rapeseed oil cake on a dry basis:

$$\begin{aligned} \text{Yield of activated carbon (wt\%)} \\ = \frac{\text{weight of activated carbon (g)}}{\text{weight of rapeseed oil cake (g)}} \times 100. \end{aligned} \quad (1)$$

Characterization of the activated carbons

Determination of specific surface areas of bio-chars and activated carbons prepared from rapeseed oil cake was done by N_2 adsorption (at 77 K) method, using a surface analyzer (Quantachrome Inst., Nova 2200e). Novawin 2

software was used to obtain results. The micropore volume (V_{micro}) was determined using the t-plot method. The mesopore volume (V_{meso}) was computed by subtracting V_{micro} from V_{total} ($V_{meso} = V_{total} - V_{micro}$).

The scanning electron microscopy (SEM) technique using a Carl Zeiss FESEM instrument was used to monitor SEM images of bio-chars and activated carbons. The isoelectric point (IEP) of the activated carbon (RAC4) was determined using a Malvern Zetasizer Nano ZS potentiometer (Malvern Instruments, UK). The pH of carbon suspensions was adjusted using 0.5 mol L⁻¹ and 0.025 mol L⁻¹ HCl or 0.1 mol L⁻¹ NaOH solutions, and the zeta potentials of RAC4 at different pH values were measured. The amounts of functional groups on the surface of RAC4 were determined according to Boehm's titration method (Boehm, 1966). The proximate analyses of rapeseed oil cake, bio-chars, and the activated carbons were carried out according to ASTM methods (D3174-04 for ash analysis and D3175-89a for volatile matter content). Elemental compositions of rapeseed oil cake, bio-chars, and activated carbons were determined by a LECO CHNS 932 Elemental Analyzer. The reported values are mean of three replicate measurements.

Adsorption experiments

The activated carbon (RAC4) was used in adsorption experiments for the removal of lead (II) and nickel (II) ions. 50 mg of the activated carbon was added to lead (II) or nickel (II) salt solutions in a closed bottle immersed in a circulating water bath at 25 °C and the adsorption media stirred using a magnetic stirrer at a continuous agitation of 150 rpm at a certain period of time to determine the optimum pH values and initial concentrations of lead (II) and nickel (II) ions. After reaching equilibriums for both ions, the adsorption medium was centrifuged and the concentration of lead (II) or nickel (II) ions in the aqueous phase was determined with an atomic absorption spectrophotometer (AAS-Perkin Elmer A. Analyst 800 Model). The amounts of lead (II) or nickel (II) ions on the adsorbent at equilibrium were calculated using the following equation:

$$q_e = \frac{(C_o - C_e)V}{W}, \quad (2)$$

where q_e (mg g⁻¹): the amount of adsorbed metal ion, C_o (mg L⁻¹): initial metal concentration in the liquid phase, C_e (mg L⁻¹): equilibrium metal ion concentration, V (L): volume of the solution, and W (g): the weight of dry adsorbent used (g).

In order to find the optimum pH for the maximum adsorption capacity of RAC4, the experiments were performed with pH ranging from 1.0 to 6.0 for lead (II) ion and 1.0 to 7.0 for nickel (II) ion. Adsorption isotherm

Table 1 Yields of prepared carbons and chemical recoveries in chemical activation process

Type of activated carbon	Activating reagent	Carbonization temperature (°C)	Yields of activated carbon* (wt %)	Chemical recovery (wt %)
RAC1	–	600	28.81	–
RAC2	–	800	26.52	–
RAC3	Na ₂ CO ₃	600	18.25	96.86
RAC4	Na ₂ CO ₃	800	11.77	95.89

* All yields calculated on a dry basis

experiments were carried out at optimum conditions (a contact time of 360 min at pH 5.0 for lead (II) ion and at pH 6.0 for nickel (II) ion) at different initial concentrations of ions (ranging from 50 to 500 ppm) at constant temperature of 25 °C.

Adsorption kinetics were determined by analyzing lead (II) and nickel (II) ions from aqueous solution at different time intervals, and the concentrations of metal ions were measured similar to those of equilibrium tests. The amount of metal ion adsorption at time t , q_t (mg g⁻¹) was computed by the following equation:

$$q_t = \frac{(C_o - C_t)V}{W}, \quad (3)$$

where C_o and C_t (mg L⁻¹) are the liquid-phase concentrations of metal ions at initial and any time t , respectively. V is the volume of the solution (L), and W is the weight of dry adsorbent used (g). The kinetic studies were performed with 50 mg of the adsorbent in 50 mL of 250 ppm lead (II) or 300 ppm nickel (II) ion solutions at constant temperature of 25 °C.

Results and discussion

Characteristics of the activated carbons

Activated carbons and bio-chars were prepared from rapeseed oil cake with and without sodium carbonate activation at 600 and 800 °C, respectively. The yields of prepared carbons and chemical recoveries of the adsorption process are presented in Table 1. The bio-char yields were found to be 28.81 and 26.52 wt % at 600 and 800 °C, respectively. The yield of bio-char slightly decreased with increasing the activation temperature from 600 to 800 °C. The yields of the activated carbons obtained at 600 and 800 °C were lower than those of corresponding bio-chars (Tay et al. 2009). Chemical recoveries in the activation process were found to be 96.86 and 95.89 wt % for RAC3

Table 2 Characteristics of the bio-chars and activated carbons prepared from Na₂CO₃ activation of rapeseed oil cake at 600 and 800 °C

Type of carbons	RAC1	RAC2	RAC3	RAC4
Proximate analysis				
Volatile matter	20.12	11.26	17.82	12.28
Fixed carbon	69.00	73.18	78.95	87.72
Ash	10.88	15.56	3.23	0.99
Elemental analysis (wt %)				
C	62.02	66.25	70.64	78.72
H	1.88	1.21	1.86	1.09
N	6.83	5.15	5.15	0.10
S	0.24	0.32	0.08	0.04
O*	29.03	27.07	22.27	20.05
Typical properties				
Specific surface area (m ² g ⁻¹)	11.98	2.95	159.74	849.55
Total pore volume (cm ³ g ⁻¹)	0.0059	0.0015	0.114	0.494
Micropore area (m ² g ⁻¹)	0	0.495	82.279	719.26
Micropore volume (cm ³ g ⁻¹)	0	0	0.033	0.324
Mesopore volume (cm ³ g ⁻¹)	0.0059	0.0015	0.081	0.170
Average pore diameter (Å)	9.83	9.97	14.31	11.62

* By difference

and RAC4, respectively. Table 2 shows the characteristics of the bio-chars and activated carbons at 600 and 800 °C. Both elemental and fixed carbon contents of activated carbons increased when the activation temperature was raised from 600 to 800 °C. The volatile matter contents of both the bio-char and activated carbon produced at 600 °C were higher than those obtained at 800 °C. The sulfur contents of the activated carbons were found to be negligible. The ash contents of activated carbons were lower than those of corresponding bio-chars produced at the same temperatures.

The specific surface areas of the bio-chars were found to be quite low. By chemical activation, the specific surface areas of the activated carbons were remarkably increased. The highest specific surface area of activated carbon (RAC4) was produced at the temperature of 800 °C, and it was found about 850 m² g⁻¹. The prepared activated carbons were mainly microporous. The micropore volume and surface area of the activated carbon increased when the carbonization temperature was raised from 600 to 800 °C. It is caused by the development of micropores on the surface of the activated carbon (Okman et al. 2014). In addition, the development of porosity of the activated carbons (RAC3 and RAC4) by Na₂CO₃ activation is associated with gasification reaction. It is assumed that

Na₂CO₃ is reduced to metallic sodium by carbon during the carbonization process according to the following reaction (Addoun et al. 2002):



The sodium metal atoms occurred during the activation stage could intercalate into the carbon structure and widen the existing pores and create new porosities (McKee 1983; Marsh and Rodríguez-Reinoso 2006).

SEM images of bio-chars (RAC1, RAC2) and activated carbons (RAC3, RAC4) are shown in Fig. 1. The surfaces of both bio-chars and activated carbons were not homogeneous. RAC1 and RAC2 surfaces have irregular cavities which are caused by releasing of volatiles from the biomass matrix. In cases of the RAC3 and RAC4, the formation of micropores on the surfaces of activated carbons was observed when the chemical activation was used. It can be seen from Fig. 1 that microporosity in RAC4 was more distinct than the RAC3 which is in agreement with the surface properties of RAC4 (Table 2). As RAC4 had the higher surface area and pore volume than other prepared carbon, the removal of lead (II) and nickel (II) ions from aqueous solution was carried out using RAC4.

Adsorption studies

Effect of pH

The pH of the solution is one of the main factors which affect the adsorption characteristics. Fig. 2 shows the effect of pH on the adsorption of lead (II) and nickel (II) ions onto RAC4. The increase of the pH of the solution up to 5.0 increased the adsorption capacity onto RAC4 for nickel (II) ions. In case of adsorption of lead (II) ions onto RAC4, the adsorption capacity increased with raising the pH of the solution up to 6.0. After these points, (pH = 6.0 for nickel (II) ions and pH = 5.0 for lead (II) ions), the adsorption capacities of RAC4 were decreased for both ions. The adsorption of metal ions is controlled by electrostatic interactions between the adsorbent and the adsorbate which depends on the carbon surface functionality (Karagoz et al. 2008; Dias et al. 2007). Surface groups of RAC4 determined by Boehm titration are shown in Table 3. Surface of the activated carbon had mainly acidic character. It is considered that metallic ion establish a complex with surface groups of RAC4 especially oxygen atoms on the surfaces. The amphoteric nature of carbon surface also depends on the isoelectric point of the carbon. Figure 3 shows the measured zeta potential as a function of solution pH for RAC4. Except for the pH = 7.5, the zeta potential of RAC4 decreased when the pH of the solution was

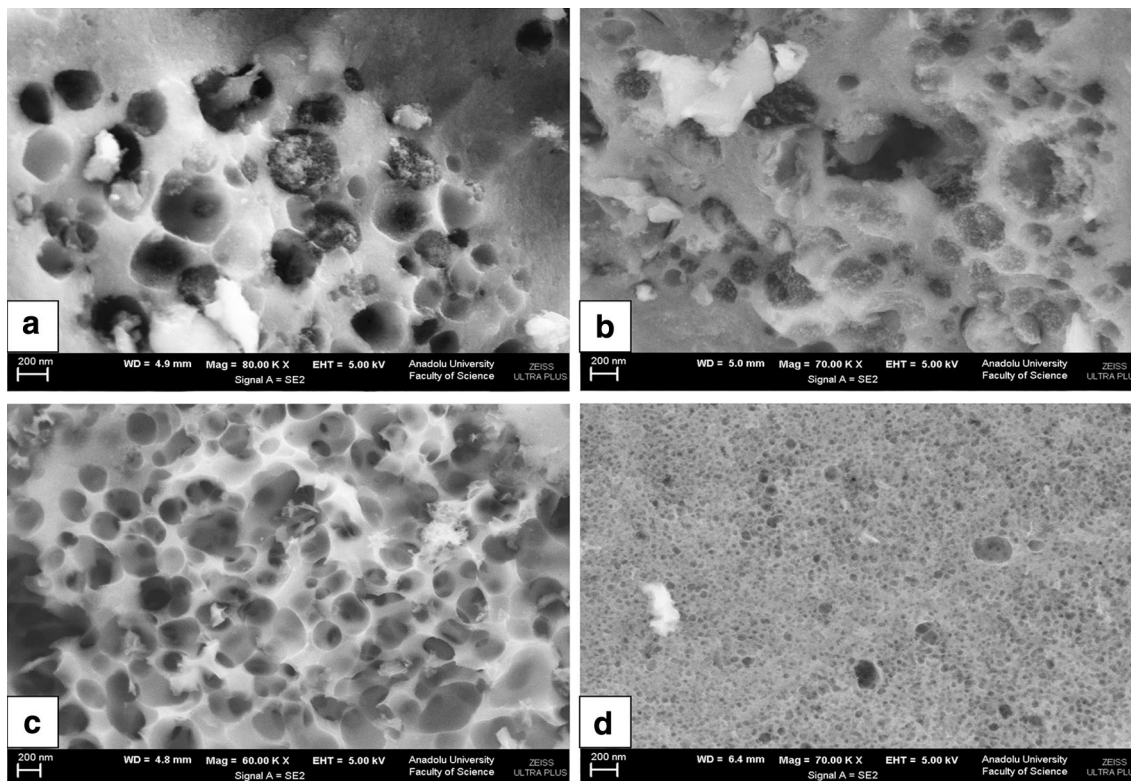


Fig. 1 SEM images of bio-chars **a** RAC1, **b** RAC2 and activated carbons **c** RAC3, **d** RAC4

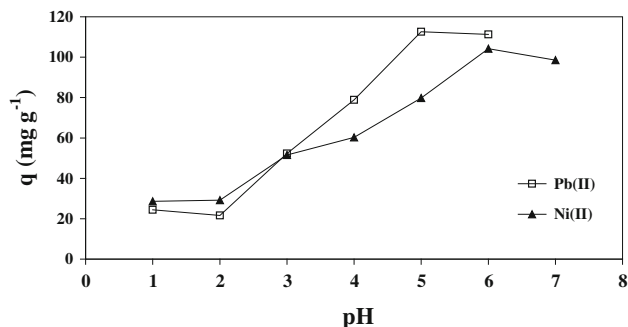


Fig. 2 Effect of pH for the adsorption of lead (II) and nickel (II) ions onto RAC4

increased. The isoelectric point of RAC4 was determined as 8.47. The high pH_{IEP} represents high basicity (Qiu et al. 2008) which may be explained the adsorption by acid base concept. Menéndez et al. stated “the isoelectric point (IEP) values are only representative for the external surface charges of carbon particles in solution” (Menéndez et al. 1995). Consequently, the effect of pH on the adsorption of lead (II) and nickel (II) ions onto the activated carbon can be explained by both chemical and electrochemical surface properties of the carbon. The maximum adsorption capacity of RAC4 was obtained at $pH = 5.0$ and $pH = 6.0$

Table 3 Surface groups of the activated carbon determined by Boehm titration

Surface Groups (meq g ⁻¹)	Carboxylic	Lactonic	Phenolic	Acidic	Basic
RAC4	3.8501	0.3028	2.1561	6.3090	3.3904

for lead (II) ions and nickel (II) ions, respectively. Thus, further adsorption experiments were carried out at these pHs (5.0 for lead (II) and 6.0 for nickel (II) ions).

Effect of contact time

Contact time experiments for the adsorption process were performed at the initial concentration of lead (II) ions (250 ppm) and nickel (II) ions (300 ppm) at 25 °C. The amount of adsorbed ions onto RAC4 versus time (0–500 min) was tested. The effect of contact time on the adsorption capacity of RAC4 for the removal of lead (II) and nickel (II) ions is shown in Fig. 4. The high proportion of the adsorption process was carried out at the first 45 min. After 100 min, there were no significant changes in the adsorption capacity of ions. The maximum adsorption capacities of RAC4 for both ions were found to be 360 min. The contact time reached to equilibriums at

Fig. 3 Zeta potentials of RAC4 as a function of pH

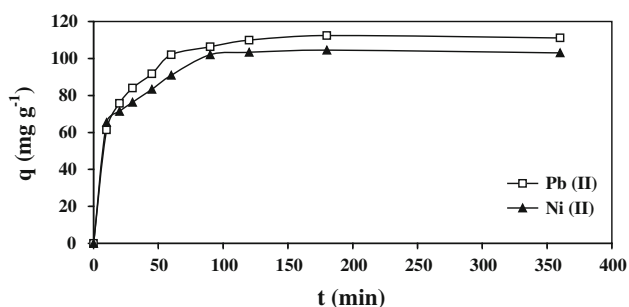
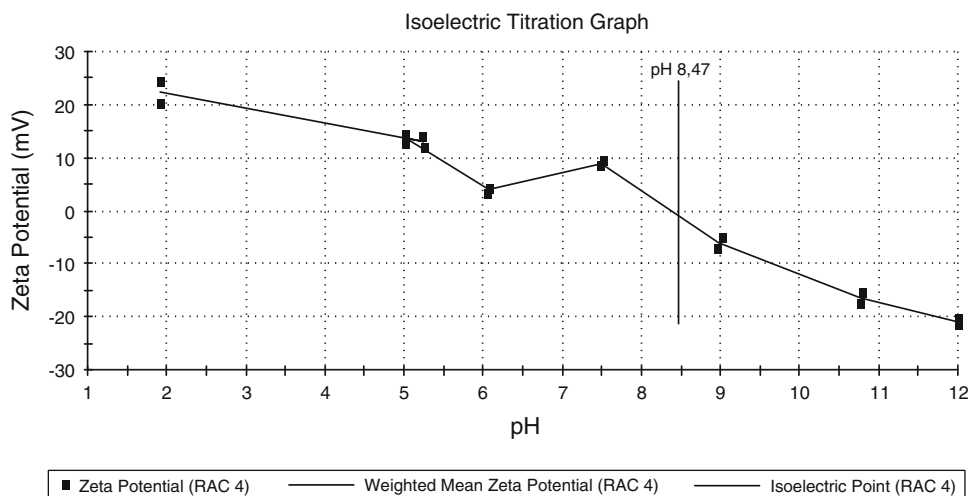


Fig. 4 The effect of contact time on the adsorption of lead (II) and nickel (II) ions onto RAC4

360 min for both tested ions. Thus, the optimum contact time was defined as 360 min for all further adsorption experiments.

Effect of initial metal ion concentration

In order to see the effect of initial metal ion concentration on the adsorption capacities of RAC4, different initial ion concentrations from 50 to 500 ppm for both tested ions were studied and shown in Fig. 5. When initial concentrations of metal ions were increased, adsorbed amount of ions on RAC4 increased due to the formation of more functional groups on the surfaces of the adsorbents (Li and Wang 2009). The amounts of adsorbed lead (II) ions were higher than those of nickel (II) ions at all initial concentrations. The optimum initial concentrations were determined as 250 and 300 ppm for lead (II) ions and nickel (II) ions, respectively.

Adsorption kinetics

The investigation of adsorption kinetics provides useful information about the adsorption process. Thus, the

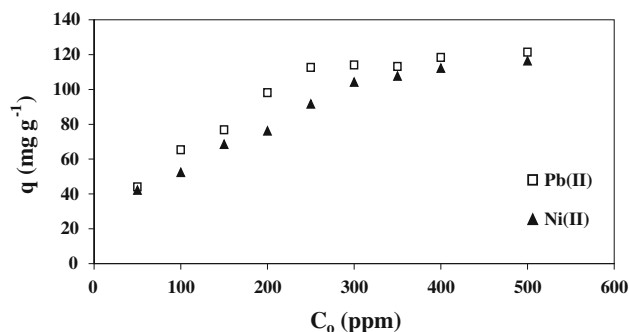


Fig. 5 Effect of initial concentration on the adsorption of lead (II) and nickel (II) ions onto RAC4

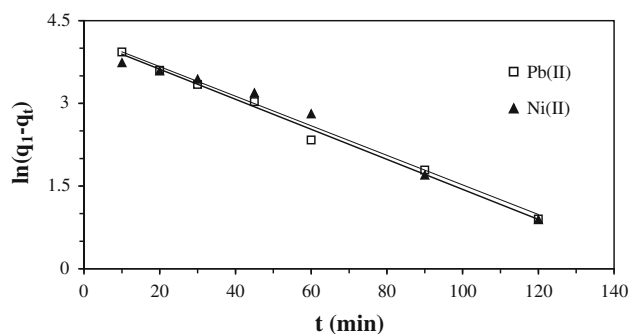


Fig. 6 Pseudo-first-order kinetic plots for the adsorption of lead (II) and nickel (II) ions onto RAC4

pseudo-first-order (Lagergren 1898), pseudo-second-order (Ho and McKay 1998) kinetic models, and intraparticle diffusion model (Weber and Morris 1963) were used to analyze adsorption kinetics for lead (II) ions and nickel (II) ions. The plots of pseudo-first-order, pseudo-second-order, and intraparticle diffusion for the adsorption of lead (II) and nickel (II) ions onto RAC4 are presented in

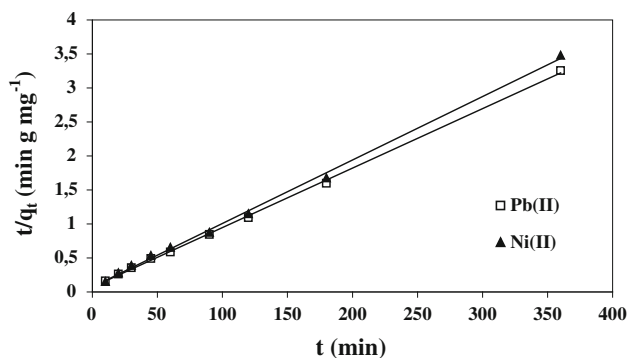


Fig. 7 Pseudo-second-order kinetic plots for the adsorption of lead (II) and nickel (II) ions onto RAC4

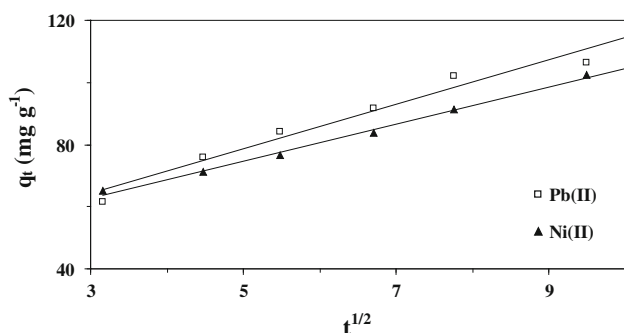


Fig. 8 Intraparticle diffusion plots for the adsorption of lead (II) and nickel (II) ions onto RAC4

Table 4 Kinetic parameters for the adsorption of lead (II) and nickel (II) ions onto RAC4 at 25 °C

Type of heavy metal	Pb(II)	Ni (II)
Pseudo-first-order		
k_1 (min ⁻¹)	0.0272	0.0268
q_1 (mg g ⁻¹)	64.23	66.75
R^2	0.9923	0.9788
Pseudo-second-order		
k_2 (g mg ⁻¹ min ⁻¹) × 10 ⁻³	0.00105	0.00115
q_2 (mg g ⁻¹)	114.94	107.53
$\frac{2}{R^2}$	0.9992	0.9982
Intraparticle diffusion		
k_p (mg g ⁻¹ min ^{-1/2})	7.1696	5.9627
C	42.659	44.875
R_p^2	0.9603	0.9935

Figs. 6, 7, and 8, respectively, and the results of kinetic parameters are given in Table 4.

The pseudo-first-order kinetic model equation according to Lagergren (1898) is expressed as

$$\ln(q_1 - q_t) = \ln q_1 - k_1 t, \quad (5)$$

where q_1 and q_t are the amounts of lead (II) or nickel (II) ions (mg g⁻¹) adsorbed at equilibrium and at time t , respectively, and k_1 is the first-order rate constant (min⁻¹).

The pseudo-second-order kinetic model (Ho and McKay 1998) is shown as

$$\frac{t}{q_t} = \frac{1}{k_2 q_2^2} + \frac{1}{q_2} t, \quad (6)$$

where q_2 is the maximum adsorption capacity (mg g⁻¹) for the pseudo-second-order adsorption and k_2 is the equilibrium rate constant for the pseudo-second-order adsorption (g mg⁻¹ min⁻¹).

The intraparticle diffusion (Weber and Morris 1963) can be illustrated by the following equation:

$$q_t = k_p t^{1/2} + C, \quad (7)$$

where C is the intercept and k_p is the intraparticle diffusion rate constant (mg g⁻¹ min^{-1/2}). According to this model, the plot of the uptake, q_t , versus the square root of time, $t^{1/2}$, is linear.

Taking into account of the correlation coefficients (R^2), the correlation coefficients for pseudo-second-order kinetic model were higher than those of the values of R^2 for the pseudo-first-order model for both lead (II) ions and nickel (II) ions. This indicates that kinetic models used for both lead (II) ions and nickel (II) ions were well fitted to the pseudo-second-order kinetic model. Previous studies concerning the adsorption of lead (II) ions and nickel (II) ions onto the activated carbon showed that the experimental data were followed pseudo-second-order kinetic model. Our results are in good agreement with these previous reports (Singh et al. 2008; Huang et al. 2011; Basso et al. 2002).

The intraparticle diffusion model is a good tool to estimate the rate-determining step. The intraparticle diffusion plots indicated single linearity for both lead (II) ions and nickel (II) ions in the adsorption process. These data show that intraparticle diffusion can play an important role. It also implies the adsorption on the external surface (migration of the solute molecules from the aqueous phase to the surface of the activated carbon) followed by diffusion into the pores. The value of R^2 for nickel (II) ions, which showed a better fit to intraparticle diffusion model, was higher than that of lead (II) ions.

Adsorption isotherms

Adsorption isotherms provide useful information about the adsorbent surface. Adsorption isotherms were studied using linear forms of Langmuir and Freundlich isotherms (Langmuir 1918; Freundlich 1906). Langmuir isotherm assumes a monolayer adsorption onto a surface, whereas

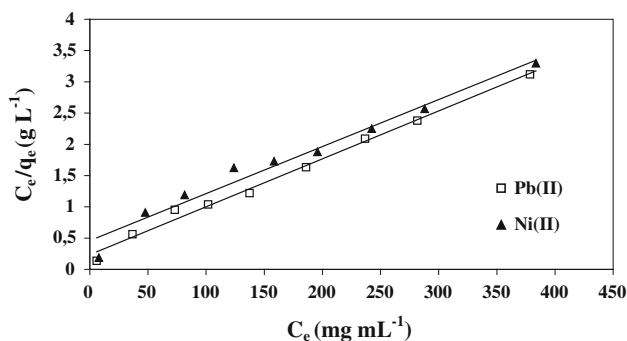


Fig. 9 Langmuir plots for the adsorption of lead (II) and nickel (II) ions onto RAC4

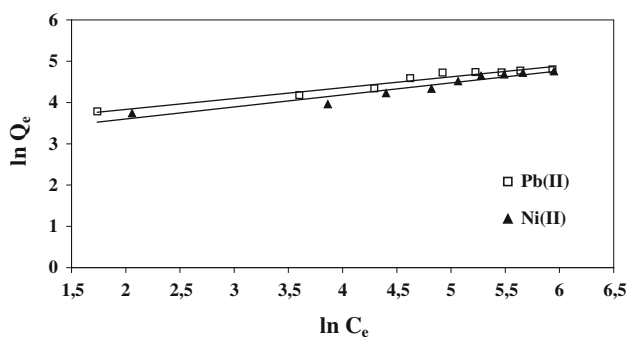


Fig. 10 Freundlich plots for the adsorption of lead (II) and nickel (II) ions onto RAC4

Freundlich isotherm describes the adsorption on heterogeneous surfaces (Adamson 1960).

$$\text{Langmuir isotherm (1918)}: \frac{C_e}{q_e} = \frac{1}{q_{\max}K_L} + \frac{C_e}{q_{\max}}, \quad (8)$$

where q_e is the equilibrium metal ion concentration on RAC4 (mg g^{-1}), C_e is the equilibrium metal ion concentration in the solution (mg L^{-1}), q_{\max} is the monolayer adsorption capacity of RAC4 (mg g^{-1}), and K_L is the Langmuir adsorption constant (L mg^{-1}). The plots of C_e/q_e versus C_e for the adsorption of metal ions onto RAC4 are shown in Fig. 9.

$$\text{Freundlich isotherm (1906)}: \log q_e = \log K_F + \frac{1}{n} \log C_e, \quad (9)$$

where q_e is the equilibrium metal ion concentration on RAC4 (mg g^{-1}), C_e is the equilibrium metal ion concentration in the solution (mg L^{-1}), K_F (L g^{-1}), and n are the Freundlich adsorption isotherm constants. The plots of \log

Table 5 Adsorption isotherms constants for the adsorption of lead (II) and nickel (II) ions onto RAC4 at 25 °C

Type of heavy metal	Pb(II)	Ni (II)
<i>Langmuir</i>		
q_{\max} (mg g^{-1})	129.87	133.33
K_L (L mg^{-1})	0.0329	0.0163
r_L^2	0.9921	0.9702
R_L	0.1084	0.1698
<i>Freundlich</i>		
n	3.807	3.422
K_F (L g^{-1})	27.32	20.40
r_F^2	0.9563	0.9251

q_e versus $\log C_e$ for the adsorption of metal ions onto RAC4 are shown in Fig. 10.

The Langmuir and Freundlich isotherm parameters for the adsorptions of lead (II) and nickel (II) ions onto RAC4 are given in Table 5. The results indicated that Langmuir isotherm was fitted the equilibrium data better than Freundlich isotherm for both adsorption of the nickel (II) and lead (II) ions onto RAC4. According to Langmuir model, there are no interactions between solute particles and carbon surfaces, and solute particles are distributed in a monolayer carbon surface. The correlation coefficients of lead (II) ions for two models were higher than those of adsorption of nickel (II) ions. RAC4 exhibited good adsorption capacity for the removal of lead (II) and nickel (II) ions. The monolayer adsorption capacities of RAC4 for the removal of lead (II) and nickel (II) ions were found to be 129.87 and 133.33 mg g^{-1} , respectively. For comparison purpose, the maximum monolayer adsorption capacities of activated carbons prepared from various lignocellulosic materials for the removal of lead (II) and nickel (II) ions from aqueous solutions are shown in Table 6. The adsorption capacities of RAC4 used in this study were comparable with other adsorbents given in the literature.

The shape of the Langmuir isotherm can also be described by a separation factor (R_L) which is defined by the following equation (Hall et al. 1966):

$$R_L = \frac{1}{1 + K_L C_o}, \quad (10)$$

where C_o is the initial concentration of metal ion (mg L^{-1}) and K_L is the Langmuir adsorption constant (L mg^{-1}).

The nature and shape of the adsorption process can be evaluated by the value of separation factor (R_L): If the R_L value is between 0 and 1, then the adsorption is favorable. If the R_L value is higher than 1, then it means that adsorption is unfavorable. The $R_L = 1$ shows linear

Table 6 Comparison for the maximum monolayer adsorption capacities of activated carbons prepared from various lignocellulosic materials for the removal of lead (II) and nickel (II) ions

Source of activated carbon	Operating conditions				Adsorption capacity (mg g ⁻¹)	
	pH	T (°C)	C _o (mg L ⁻¹)	Dosage(g L ⁻¹)	Pb(II)	Ni (II)
Hazelnut husks (Imamoglu and Tekir 2008)	5.7	18	200	12.0	13.05	
Coconut shell (Song et al. 2010)	3.2–3.6	25	20–260	2.0	40.10	
Palm shell (Issabayeva et al. 2006)	5.0	27	100–700	5.0	95.20	
Tamarind wood (Singh et al. 2008)	6.5	25	40	3.0	134.22	
Lotus stalk (Liu et al. 2013)	5.0	22	60–250	0.3	240.60	
Rapeseed oil cake (present study)	5.0	25	250	1.0	129.87	
Sugarcane bagasse pith (Anoop Krishnan et al. 2011)	6.5	30	50–1000	2.0		140.85
Coirpith (Kadirvelu et al. 2001)	5.0	30	10–40	0.4		62.50
Parthenium (Kadirvelu et al. 2002)	5.0	20	10–70	1.0		54.35
Almond husk (Hasar 2003)	5.0	20	25	5.0		37.17
Almond shell (Kılıç et al. 2013)	7.0	40	100	7.0		22.22
Rapeseed oil cake (present study)	6.0	25	300	1.0		133.33

adsorption, and the $R_L = 0$ indicates irreversible adsorption. In the present study, the values of R_L for the adsorptions of the lead (II) and nickel (II) ions onto RAC4 were in the range of 0–1 (Table 5). Thus, the adsorption process for the removal of lead (II) and nickel (II) ions from aqueous solutions is favorable.

Conclusions

The activated carbons were prepared from rapeseed oil cake with chemical activation by Na₂CO₃ at 600 and 800 °C in the study. The prepared activated carbons had a microporous nature. The activated carbon with the highest surface area of 850 m² g⁻¹ was obtained at 800 °C. It was used for the removal of lead (II) and nickel (II) ions from aqueous solutions. The maximum adsorption capacity of the activated carbon was obtained at pH 5.0 and pH 6.0 for lead (II) ions and nickel (II) ions, respectively. Kinetic evaluations for both ions showed that the experimental data were well fitted to pseudo-second-order model with the correlation coefficients of higher than 0.99. The adsorption data for both tested ions were well fitted to Langmuir isotherm. The maximum monolayer adsorption capacities of RAC4 for the removal of lead (II) and nickel (II) ions were found to be 129.87 and 133.33 mg g⁻¹, respectively.

Consequently, activated carbon was successfully prepared from agricultural by-product and used for the removal of heavy metal ions from aqueous solutions. The production of low-cost adsorbents from agricultural by-products and their use for removal of heavy metal ions are important from environmental and economic viewpoints.

Acknowledgments This study was supported by Dokuz Eylül University, Anadolu University, and Karabük University.

References

- Adamson AW (1960) Physical Chemistry of Surface. Interscience Publication, New York
- Addoun A, Dentze J, Ehrburger P (2002) Porosity of carbons obtained by chemical activation: effect of the nature of the alkaline carbonates. Carbon 40(7):1140–1143
- Amin MN, Mustafa AI, Khalil MI, Rahman M, Nahid I (2012) Adsorption of phenol onto rice straw biowaste for water purification. Clean Technol Environ Policy 14:837–844
- Anoop Krishnan K, Sreejalekshmi KG, Baiju RS (2011) Nickel (II) adsorption onto biomass based activated carbon obtained from sugarcane bagasse pith. Biores Technol 102:10239–10247
- Bacaoui A, Yaacoubi A, Dahbi A, Bennouna C, Phan Tan Luu R, Maldonado-Hodar FJ, Rivera-Utrilla J, Moreno-Castilla C (2001) Optimization of conditions for the preparation of activated carbons from olive-waste cakes. Carbon 39:425–432
- Basso MC, Cerella EG, Cukierman AL (2002) Activated carbons developed from a rapidly renewable biosource for removal of Cadmium (II) and Nickel (II) Ions from dilute aqueous solution. Ind Eng Chem Res 41:180–189
- Boehm HP (1966) Chemical identification of surface groups. Adv Catal 16:179–274
- Chouchene A, Jeguirim M, Trouve G (2014) Biosorption performance, combustion behavior, and leaching characteristics of olive solid waste during the removal of copper and nickel from aqueous solutions. Clean Technol Environ Policy 16:979–986
- Cimino G, Cappello RM, Caristi C, Toscano G (2005) Characterization of carbons from olive cake by sorption of wastewater pollutants. Chemosphere 61:947–955
- Dias JM, Alvim-Ferraz MCM, Almeida MF, Rivera-Utrilla J, Sánchez-Polo M (2007) Waste materials for activated carbon preparation and its use in aqueous-phase treatment: a review. J Environ Manag 85:833–846

- El-Ashtoukhya ESZ, Amin NK, Abdelwahabb O (2008) Removal of lead (II) and copper (II) from aqueous solution using pomegranate peel as a new adsorbent. *Desalination* 223:162–173
- Freundlich HMF (1906) Over the adsorption in solution. *J Phys Chem* 57:385–471
- Giraldo-Gutierrez L, Moreno-Pirajan JC (2008) Pb(II) and Cr(VI) adsorption from aqueous solution on activated carbons obtained from sugar cane husk and sawdust. *J Anal Appl Pyrolysis* 81:278–284
- Hall KR, Eagleton LC, Acrivos A, Vermeulen T (1966) Pore- and solid-diffusion kinetics in fixed-bed adsorption under constant-pattern conditions. *Ind Eng Chem Fundam* 5:212–223
- Haroun AA, El-Halawany NR (2011) Preparation and evaluation of novel interpenetrating polymer network-based on newspaper pulp for removal of copper ions. *Polym-Plast Technol* 50:232–238
- Haroun AA, Mashaly HM, El-Sayed NH (2013) Novel nanocomposites based on gelatin/HPET/chitosan with high performance acid red 150 dye adsorption. *Clean Technol Environ Policy* 15:367–374
- Hasar H (2003) Adsorption of nickel (II) from aqueous solution onto activated carbon prepared from almond husk. *J Hazard Mater* B97:49–57
- Hebeish A, Ramadan MA, Abdel-Halim E, Abo-Okeil A (2011) An effective adsorbent based on sawdust for removal of direct dye from aqueous solutions. *Clean Technol Environ Policy* 13:713–718
- Ho YS, McKay G (1998) Kinetic models for the sorption of dye from aqueous solution by wood. *Process Saf Environ Prot* 76:183–191
- Huang L, Sun Y, Yang T, Li L (2011) Adsorption behavior of Ni (II) on lotus stalks derived active carbon by phosphoric acid activation. *Desalination* 268:12–19
- Imamoglu M, Tekir O (2008) Removal of copper (II) and lead (II) ions from aqueous solutions by adsorption on activated carbon from a new precursor hazelnut husks. *Desalination* 228:108–113
- Ioannidou O, Zabaniotou A (2007) Agricultural residues as precursors for activated carbon production—A review. *Renew Sust Energy Rev* 11:1966–2005
- Ismadji S, Sudaryanto Y, Hartono SB, Setiawan LEK, Ayucitra A (2005) Activated carbon from char obtained from vacuum pyrolysis of teak sawdust: pore structure development and characterization. *Biores Technol* 96:1364–1369
- Issabayeva G, Aroua MK, Sulaiman NMN (2006) Removal of lead from aqueous solutions on palm shell activated carbon. *Biores Technol* 97:2350–2355
- Kadirvelu K, Thamaraiselvi K, Namasivayam C (2001) Adsorption of nickel (II) from aqueous solution onto activated carbon prepared from coirpith. *Sep Purif Technol* 24:497–505
- Kadirvelu K, Senthilkumar P, Thamaraiselvi K, Subburam V (2002) Activated carbon prepared from biomass as adsorbent: elimination of Ni(II) from aqueous solution. *Bioresour Technol* 81:87–90
- Karagoz S, Tay T, Ucar S, Erdem M (2008) Activated carbons from waste biomass by sulfuric acid activation and their use on methylene blue adsorption. *Biores Technol* 99:6214–6222
- Kardam A, Raj KR, Srivastava S, Srivastava MM (2014) Nanocellulose fibers for biosorption of cadmium, nickel, and lead ions from aqueous solution. *Clean Technol Environ Policy* 16:385–393
- Kılıç M, Kırbiyık Ç, Çepeliogullar Ö, Pütün AE (2013) Adsorption of heavy metal ions from aqueous solutions by bio-char, a by-product of pyrolysis. *Appl Surf Sci* 283:856–862
- Lagergren S (1898) Zur theorie der sogenannten adsorption gelöster stoffe. *Kungliga Svenska Vetenskapsakademiens Handlingar* 24(4):1–39
- Langmuir I (1918) The adsorption of gases on plane surfaces of glass, mica and platinum. *J Am Chem Soc* 40:1361–1403
- Li K, Wang X (2009) Adsorptive removal of Pb(II) by activated carbon prepared from *Spartina alterniflora*: equilibrium, kinetics and thermodynamics. *Biores Technol* 100:2810–2815
- Li S, Xu S, Liu S, Yang C, Lu Q (2004) Fast pyrolysis of biomass in free-fall reactor for hydrogen-rich gas. *Fuel Process Technol* 85:1201–1211
- Liu H, Dai P, Zhang J, Zhang C, Bao N, Cheng C, Ren L (2013) Preparation and evaluation of activated carbons from lotus stalk with trimethyl phosphate and tributyl phosphate activation for lead removal. *Chem Eng J* 228:425–434
- Marsh H, Rodríguez-Reinoso F (2006) *Activation Processes (Chemical) Activated Carbon*. Elsevier Ltd, Oxford, pp 322–365
- McKee DW (1983) Mechanisms of the alkali metal catalyzed gasification of carbon. *Fuel* 62:170–175
- Menéndez JA, Illán-Gómez MJ, y León CAL, Radovic LR (1995) On the difference between the isoelectric point and the point of zero charge of carbons. *Carbon* 33:1655–1659
- Merrikhpour H, Jalali M (2013) Comparative and competitive adsorption of cadmium, copper, nickel, and lead ions by Iranian natural zeolite. *Clean Technol Environ Policy* 15:303–316
- Nethaji S, Sivasamy A (2014) Removal of hexavalent chromium from aqueous solution using activated carbon prepared from walnut shell biomass through alkali impregnation processes. *Clean Technol Environ Policy* 16:361–368
- Okman I, Karagöz S, Tay T, Erdem M (2014) Activated carbons from grape seeds by chemical activation with potassium carbonate and potassium hydroxide. *Appl Surf Sci* 293:138–142
- Patterson JW (1985) *Industrial Wastewater Treatment Technology*, 2nd edn. Butterworth Publishers, London
- Qiu Y, Cheng H, Xu C, Sheng GD (2008) Surface characteristics of crop-residue-derived black carbon and lead (II) adsorption. *Water Res* 42:567–574
- Sentorun-Shalaby C, Ucak-Astarlioglu MG, Artok L, Sarici C (2006) Preparation and characterization of activated carbons by one-step steam pyrolysis/activation from apricot stones. *Microporous Mesoporous Mat* 88:126–134
- Singh CK, Sahu JN, Mahalik KK, Mohanty CR, Mohan BR, Meikap BC (2008) Studies on the removal of Pb(II) from wastewater by activated carbon developed from Tamarind wood activated with sulphuric acid. *J Hazard Mater* 153:221–228
- Song X, Liu H, Cheng L, Qu Y (2010) Surface modification of coconut-based activated carbon by liquid-phase oxidation and its effects on lead ion adsorption. *Desalination* 255:78–83
- Sudaryanto Y, Hartono SB, Irawaty W, Hindarso H, Ismadji S (2006) High surface area activated carbon prepared from cassava peel by chemical activation. *Biores Technol* 97:734–739
- Tay T, Ucar S, Karagöz S (2009) Preparation and characterization of activated carbon from waste biomass. *J Hazard Mater* 165:481–485
- Visa M, Pricop F, Duta A (2011) Sustainable treatment of wastewaters resulted in the textile dyeing industry. *Clean Technol Environ Policy* 13:855–861
- Weber WJ, Morris JC (1963) Kinetics of adsorption on carbon from solution. *J Sanit Eng Div* 89:31–60
- Yalçın N, Sevinç V (2000) Studies of the surface area and porosity of activated carbons prepared from rice husks. *Carbon* 38:1943–1945
- Zhang J, Jin L, Zhu S, Hu H (2012) Preparation of mesoporous activated carbons from coal liquefaction residue for methane decomposition. *J Nat Gas Chem* 21:759–766